# Local electronic structure of ZnS and ZnSe doped by Mn, Fe, Co, and Ni from x-ray-absorption near-edge structure studies

K. Ławniczak-Jabłonska, R. J. Iwanowski, and Z. Gołacki
*Institute of Physics, Polish Academy of Sciences, Al.Lotników 32/46, PL-02-668 Warsaw, Poland*

A. Traverse, S. Pizzini, and A. Fontaine
*Laboratoire pour l'Utilisation du Rayonnement Electromagnetique, Universite de Paris-Sud, Batiment 209D, F-91405 Orsay, Cedex, France*

I. Winter and J. Hormes
*Physikalisches Institut der Universitat Bonn, Nussallee 12, D-5300 Bonn 1, Germany*
(Received 3 May 1995)

Systematic studies of x-ray-absorption near-edge structure (XANES) at the $K$ edge of cations and anions in ZnS, ZnSe, and Zn$M$S and Zn$M$Se compounds, with $M$ being a transition metal (Mn, Fe, Co, Ni), were performed. Our investigations have shown, in agreement with earlier literature results of multiple-scattering theory, that the distribution of unoccupied $p$-like states around cation atoms is mainly determined by the type of anion and does not depend significantly on the $M$ concentration. Three peak structures can be found in the cation $K$-edge XANES of the sulphides, whereas a two-peak structure is observed in selenides. The effective charge transfer for the $M$ cation was estimated within 2–2.5$e$, from measured chemical shifts of the respective $K$ edges. Additionally, direct evidence of hybridization between the states of $M$ and $p$ states of S was found from S $K$-edge XANES studies. The empirical correlation between the shape of $M$ $K$ edges and the solubility limit of $M$ in the investigated solid matrices was revealed.

## I. INTRODUCTION

For more than two decades numerous studies have been concentrated on II-VI compounds doped with transition metals ($M's$) (e.g., Refs. 1 and 2). These compounds belong to an intermediate class of materials, so-called diluted magnetic semiconductors (DMS's), which have been classified between nonmagnetic and magnetic semiconductors. DMS's exhibit properties dissimilar to those of host II-VI compounds. The differences are due to substitution of the group-II metal by a magnetic ion (here $M$), which occurs in the cation sublattice. The very special properties of $M$ are caused by narrow partly filled $3d$ bands. Hybridization of $3d$ states of $M$ with the $sp$-band states of a host II-VI semiconductor inevitably induces a modification of the crystal band structure and gives rise to electronic and magnetic properties of physical and technological interest. Earlier investigations of the II-VI-based DMS's concerned mainly the case of Mn (Refs. 1 and 2) or Fe doping,[3,4] although the last years brought an extension of scientific interest over the II-VI DMS containing the other transition metals, like Co or Ni (see, e.g., Refs. 5–7).

Among different experimental methods, x-ray-absorption spectroscopy has also been involved there. This included both the EXAFS (extended x-ray-absorption fine structure) and XANES (x-ray-absorption near-edge structure) investigations. EXAFS, which provides information on the geometric structure (interatomic distances, coordination numbers) around the absorbing atoms,[8] has also become a useful technique for structural investigations in the case of DMS's (see, e.g., Refs. 9–12). On the other hand, XANES, which potentially contains information about the local electronic structure and about the geometrical arrangement of atoms around the absorbing center,[13] was rather rarely applied in the studies of DMS's (e.g., Refs. 14–16). Two types of XANES interpretation can be found in the literature. The first, relying on use of the multiple-scattering (MS) theory (e.g., Ref. 17) and the second, based on the band-structure calculations extended toward large kinetic energy of the photoelectrons.[18] Both methods have produced results consistent with the experimental spectra (see Ref. 19 and references therein). Despite a complexity of theoretical description of XANES spectra, there also exists a phenomenological approach which treats the shape of the XANES curve as a fingerprint for certain types of chemical bonding (e.g., Refs. 20 and 21). Under the assumption of a single-particle model, and due to selection rules, direct information about the local density of states around emitting atom, in our case $p$-like unoccupied states, can be deduced. It seems obvious that such an approach requires collecting systematic experimental evidence for the compounds of interest.

Due to the lack of such evidence the goal of our paper is to investigate the evolution of XANES at the $K$ edges in the $Zn_{1-x}M_xA$ compounds, with the following parameters: (i) the anion type ($A$ being S or Se), (ii) the $M$ cation type ($M$ being Mn, Fe, Co, Ni), and (iii) $M$ concentration $x$. In particular, our interest concerned the following topics.

(i) Variation of an energy distribution of the density of unoccupied $p$-like states around the Zn atom with a concentration of the $M$ dopant in ZnS and ZnSe, and with filling of the $3d$ band in $M$, when stepping up from Mn to Ni.

(ii) The distribution of the $p$-like state densities around $M$ in both matrices and its change with the $M$ content.

(iii) The influence of anion type (S, Se) on the shape of

 

TABLE I. List of the DMS crystals used in recent experiment. Solid solubility limits of particular transition metals in ZnS and ZnSe have been inserted in square brackets. ($w$) is the wurtzite structure (the other crystals have a zinc-blende structure).

| | M content ($x$) | | | |
|---|---|---|---|---|
| Alloy | Mn | Fe | Co | Ni |
| $Zn_{1-x}M_xS$ | [0.60][a] | [0.58][b] | [0.44][c] | [0.03][d] |
| | 0.33 ($w$) | 0.50 | 0.25 | 0.01 |
| | 0.20 ($w$) | 0.24 | 0.16 | |
| | 0.12 ($w$) | 0.11 | 0.10 | |
| $Zn_{1-x}M_xSe$ | [0.57][e] | [0.25][f] | [0.18][g] | [0.02][h] |
| | 0.37 | 0.18 | 0.07 | 0.01 |
| | 0.21 | 0.08 | 0.02 | 0.005 |

[a]Reference 2. [e]Reference 23.
[b]Reference 22. [f]Reference 4.
[c]Reference 25. [g]Reference 6.
[d]Reference 7. [h]Reference 24.

cation $p$-like state distributions for both groups of compounds studied.

(iv) Possible correlations between the energy distribution of $p$-like state densities of particular transition metals in the compounds studied, and the solid solubility limit of $M$ in these II-VI matrices.

(v) The influence of substitution within the nearest neighbors of anions on the distribution of $p$ states around the Se or S atoms.

## II. EXPERIMENT

$Zn_{1-x}M_xS$ and $Zn_{1-x}M_xSe$ ($M$=Mn, Fe, Co, Ni) mixed crystals were grown at the Institute of Physics, Polish Academy of Sciences. The ternary compounds containing Co and Ni were prepared by chemical vapor transport using iodine as a transport agent.[2] Solid solutions containing Fe or Mn as admixed elements were grown by the triple sintering of ZnS and ZnSe with appropriate monochalcogenides of transition metals at 1200 °C.

A complete list of the DMS crystals used in this experiment was given in Table I. The composition of these alloys ($x$) has been precisely determined with use of electron microprobe Jeol JSM-50A. X-ray-diffraction studies were performed by a conventional x-ray powder diffractometer (Cu $K\alpha$ radiation). Besides the $Zn_{1-x}Mn_xS$ samples, which crystallize in a wurzite structure [denoted by ($w$) in Table I], the rest of the crystals studied had a zinc-blende structure. The diffractograms showed no traces of the other phase and/or $M$ precipitations. Each atom in the wurzite and zinc-blende structure has four nearest neighbors. These structures differ only slightly in the parameters of the unit cell, which is hexagonal in the case of wurzite and cubic in the case of zinc blende.

The solubility of $M$ in the matrices under study decreases drastically with rise of the $M$ $3d$-band filling, falling down to less than 2 at % in the case of Ni in selenides, and remains systematically higher in sulphides than in selenides. For comparison, the known values of solid solubility limits of particular $M$ dopants in ZnS and ZnSe have been inserted in square brackets in Table I.

For reference purpose of the XANES experiment, we have also prepared the following $M$ monochalcogenides: MnS, FeS, CoS, NiS, MnSe, FeSe, CoSe, and NiSe. All these compounds crystallized in the NiAs structure (type $B13$), except for the Mn compounds which had NaCl structure (type $B1$). In both structures each atom is surrounded by six nearest neighbors.

The XANES at the $K$ edge of $M$, Zn, and Se have been recorded at room temperature in the transmission or fluorescence mode using synchrotron radiation at the (x-ray-absorption spectroscopy) XAS1 station of the DCI ring at Laboratoire pour L'Utilisation du Rayonnement Electromagnetique, Orsay, France. The Si(331) channel-cut crystal monochromator provided a spectral range of 6–30 keV with an energy resolution of $\Delta E/E \sim 10^{-4}$. The storage ring was operating at $E=1.85$ GeV, with a beam current ranging within 200–300 mA. The XANES data range was usually fixed between $-30$ and 100 eV (referred to the $K$-edge position), and were collected in 0.5- or 0.8-eV steps.

Following the requirements of x-ray-absorption measurements in the transmission mode for higher energies, the crystals studied were powdered and subsequently mixed with cellulose powder and then pressed to form homogeneous pellets of uniform thickness. The optimum specimen thickness for measuring the $K$ edges was chosen to meet the condition $\mu d = -\ln I/I_0 \sim 1$, where $\mu$ is the sample linear absorption coefficient, $d$ is the sample thickness, and $I$ and $I_0$ are the measured intensities after and before the sample, respectively. We obtained well-pronounced edges for the samples prepared in this way when their mass did not exceed 40 mg/cm$^2$. This condition has been fulfilled for all sulfides except of the Ni $K$-edge measurement in $Zn_xNi_{1-x}S$, where the $M$ concentration was too small and fluorescence detection became necessary. For selenides, all $K$ edges of Se and Zn were measured in the transmission mode, whereas only Mn and Fe $K$ edges were well visible in transmission. For lower $M$ content, i.e., $x \leqslant 0.07$ (the cases of Co and Ni in ZnSe—see Table I) the amount of material was too large to prepare the homogeneous samples, and the fluorescence mode was applied. Also, the effect of reabsorption was not noticed in the XANES spectra. For measurements in the fluorescence mode, the crystalline powder was directly deposited on the Scotch tape attached to the sample holder. The higher harmonics content of the beam was suppressed, and we have not made any additional verification of the spectra in the XANES range for harmonics.

It should be added here that for the samples with low $M$ concentration ($x \leqslant 0.07$) we have also carried out complementary measurements of the $M$ $K$ edge in the total electron yield mode. However, one failed to obtain better XANES spectra than in the case of the fluorescence mode—hence we resigned from presenting them in our report. For each set of $K$-edge XANES runs the energy scale was calibrated by a measurement of the corresponding pure element ($M$, Zn, Se) as reference.

X-ray-absorption measurements at the sulfur $K$ edge were acquired at the BN3 beamline of the Electron Stretcher Accelerator ELSA in Bonn. The storage ring operated at 2.3 GeV with an average electron current of about 35 mA. The synchrotron radiation was monochromatized with a

Lemmonier-type double-crystal monochromator,[26] equipped with InSb(111) crystals, giving a resolution of 1 eV at the S $K$ edge. The spectra were measured in standard transmission mode: two ionization chambers filled with air monitored the photon beam intensity before and after the sample.[27] The first strong resonance in the spectrum of $ZnSO_4$ at 2481.44 eV was used as a "secondary" energy standard, which was precisely calibrated against the $1s$-$4p$ Rydberg transition in argon gas at an energy of 3203.54 eV.[28] The samples were powdered and placed on 20-$\mu$m-thick polyimide film.

## III. RESULTS AND INTERPRETATION

### A. X-ray absorption at the Zn $K$ edge

In this section we present the experimental $K$-edge absorption spectra of the Zn cation in DMS alloys based on ZnS and ZnSe. Here we shall discuss only XANES in the energy range up to ~50 eV above the edge. The results of an EXAFS study for Co in the ZnS and ZnSe matrices have been already published.[29] An analogous EXAFS analysis for the other $M$'s in these matrices is under preparation.

Figures 1(a) and 1(b) present the $K$-edge XANES spectra of Zn for $Zn_{1-x}M_xS$ and $Zn_{1-x}M_xSe$, respectively. Each figure includes the set of Zn $K$-edge absorption spectra which are representative of ZnS and ZnSe alloyed with respective $M$'s (here Mn, Fe, and Co). On the other hand, the $K$-edge XANES spectra of Zn in $Zn_xFe_{1-x}S$ and $Zn_xCo_{1-x}Se$, for different $M$ contents, are exposed as an example in Figs. 2(a) and 2(b), respectively.

It can be seen from the above figures that there is no chemical shift between Zn $K$ edges in the compounds with different $M$'s. The characteristic shape of host cation (Zn) $K$-edge XANES, and thus the energy distribution of the $p$-like state densities, is mainly determined by the type of anion (here S or Se). It also remains practically independent of the $M$ concentration (Fig. 2). The Zn $K$-edge XANES in sulfides display three well-defined peaks ($A$, $B$, and $C$), whereas it displays only two peaks ($A$ and $B$) in selenides. The nearest neighbors of each Zn atom remain unchanged (four S or Se atoms) with admixing $M$. Our EXAFS study[29] revealed that, within the accuracy of this technique, the distance between the Zn atom and respective anion (S or Se) remains unchanged with the growing content of $M$ (here Co) up to its solubility limit {$d$(Zn-S)=2.344 Å, $d$(Zn-Se)=2.455 Å, with an error of $\mp$0.005 Å}. Substitution of the host cation by a $M$ atom changes the second neighbors of Zn. Within the accuracy of our measurements, second neighbors do not influence the shape of the resonances in the Zn $K$-edge XANES. The only change observed with rising $M$ content is the increase in strength of the resonances, seen particularly well in the case of maximum $A$ (see Fig. 2). The $K$-edge XANES here reproduces the density distribution of the unoccupied $p$-like states around Zn atoms. Reduction of the Zn atomic content causes an increased localization of the Zn $p$-like states and, in consequence, sharper resonances. All spectra of Zn were measured in the transmission mode, and the amount of material used for pellet preparation fulfilled the same absorption condition (Sec. II)—therefore the above phenomenon, observed for each $M$, cannot be related with a sample thickness effect.

The experimental data presented are consistent with the results of MS calculations of the Zn $K$-edge XANES spectra

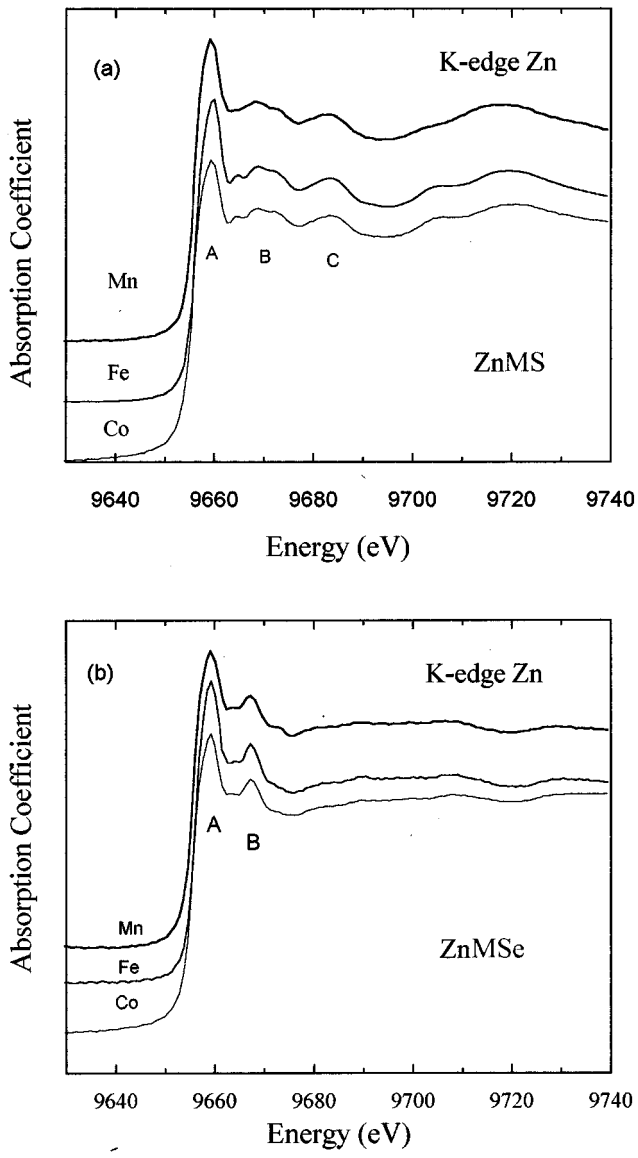


FIG. 1. $K$ edges of Zn atoms in (a) $Zn_{1-x}M_xS$, Co—$x$=0.25, Fe—$x$=0.24, and Mn—$x$=0.20; and (b) $Zn_{1-x}M_xSe$, Co—$x$=0.07, Fe—$x$=0.18, and Mn—$x$=0.21.

performed for ZnS.[17,30] In these studies the influence of a number of the coordination shells, taken into account in MS calculations, has been discussed in detail. Due to the fact that the amplitude of photoelectron scattering on the Zn and $M$ atoms is much smaller than for scattering on the S atoms, the main features of the Zn $K$-edge structure (i.e., three peaks, denoted by us as $A$, $B$, and $C$) are already replicated after scattering on the atoms of the first coordination sphere.[30] Addition of the second shell with 12 Zn atoms does not practically add features, but only increases the amplitude of the existing ones, whereas inclusion of the third shell with anion atoms contributes to the details of the near-edge structure.[30] After incorporating five shells, the best fit to the experimental data was reached[17] (see also Ref. 30). Furthermore, if in the second shell of Zn neighbors the host cation is substituted by a $M$ with a small scattering amplitude, no significant changes of the XANES features can be expected. This remains in agreement with our recent observation.

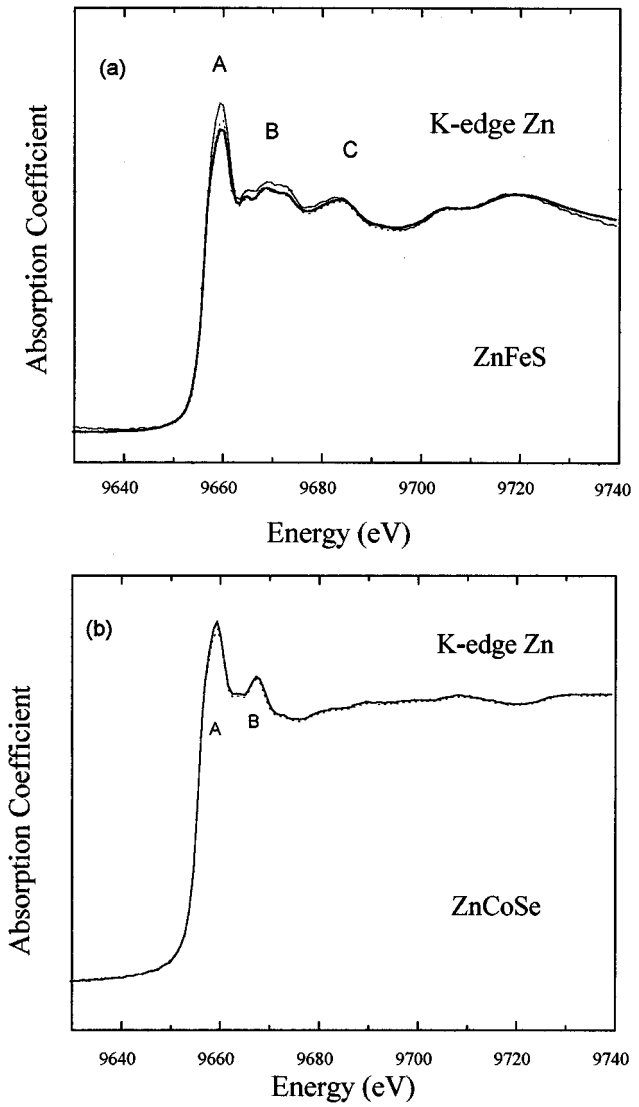


FIG. 2. *K* edges of Zn atoms in (a) $Zn_{1-x}Fe_xS$, $x=0.50$ (thin solid line), $x=0.24$ (dashed line), and $x=0.11$ (thick solid line); and (b) $Zn_{1-x}Co_xSe$, $x=0.07$ (solid line) and $x=0.02$ (dashed line).

### B. X-ray absorption at the *M K* edges

The *K*-edge XANES spectra of the chosen transition metals (Mn, Fe, Co, Ni) alloyed with ZnS or ZnSe in various atomic compositions ($x$) were collected in Figs. 3 and 4, respectively. For comparison, the *M K*-edge XANES plots of the respective *M* monochalcogenides were also inserted there.

It can be seen from the above figures that the *K*-edge XANES of the *M* reveal the structure, which shows similarity and direct correspondence with the three- or two-peaks structures characteristic of the Zn XANES in the alloys studied (see Fig. 1), and differs considerably from the *K*-edge spectra typical of elemental *M* (e.g., Ref. 20) or for *M* chalcogenides. In fact, transition metals crystallize in the closely packed structure with eight or 12 nearest neighbors, whereas *M* chalcogenides (with Fe, Co, or Ni) form a NiAs or NaCl structure (in the case of Mn)—in both latter structures each atom is octahedrally coordinated. On the other hand, the *M* atom in ZnS or ZnSe is tetrahedrally coordinated by S or Se atoms, and their distance, within the accuracy of EXAFS, remains constant with the *M* concentration.[29] Generally, the shape of *M* XANES resonances does not change with alloy composition, although with rising *M* content they tend to become less sharp, thus indicating a decrease of the *M*-related *p*-state localization. This is especially seen in Fig. 3(b), where the Fe content reaches $x=0.50$. All Fe spectra were measured in the transmission mode. The effect of smoothing the shape of the resonances was noticeable irrespective of the thickness effect, which significantly influenced the edge-height-to-background ratio.

A similar dependence of the edge structure on the absorber coordination has been observed by McKeown[17] in the *K*-edge XANES of Zn in ZnS and of Cu and Fe in chalcopyrite ($CuFeS_2$). All these three cations are nearly identically coordinated, and their XANES spectra have similar features. It was proved by the MS calculations performed in Ref. 17 that the main distinction in the shape of their *K* edges results from different atomic contributions to the x-ray-absorption cross section. For $FeS^{5-}_4$, $CuS^{6-}_4$, and $ZnS^{6-}_4$ clusters, the calculated x-ray-absorption atomic cross section develops a sharp maximum above the edge as the atomic number of the absorbing cation increases. The slope of the edge maximum and the energy extent of the edge jump depends on the absorber atom. That is, for the Zn *K* edge it extends only 5 eV at the sharpest, whereas for Cu and Fe the edge jump develops over 20 eV. This could explain the main qualitative differences observed by us between the intensity and shape of feature *A* in the *K* edge of Zn and *M* in the DMS's studied.

A detailed analysis of the fine structure of the *M K*- absorption edges provides useful information about the density distribution of *p*-like states, including these spectral features that are characteristic for each *M* but independent of the type of solid matrix. This is the case for the so-called preedge absorption feature (marked by an arrow in Figs. 3 and 4) which is widely known as being characteristic only of transition metals (e.g. Refs. 20, 31, and 32). This structure was usually assigned to a $1s$-$3d$ atomic transition (e.g. Refs. 31 and 32). The amplitude of the preedge feature does not depend on the content and type of the *M* (see Fig. 5) in all tetrahedrally coordinated compounds studied here, but is considerably smaller in octahedrally coordinated monochalcogenides (Figs. 3 and 4). Similar effect have been reported in Mn compounds.[33] This suggests that the nature of the preedge feature should rather be ascribed to the transition of the $1s$ electron of the absorber to the bound state induced by hybridization of the cation and anion states, although in consistency with its (preedge) independence of the choice of transition metal (the filling of the $3d$ band increases from Mn to Ni) and its concentration, which influences the overlapping of the *M* orbitals. It can be clearly seen in Fig. 5 that only the distance between the preedge and edge positions ($E_0$) increases with the $3d$- band filling in *M*. Furthermore, our observation also coincides with the suggestion from Ref. 17 that the preedge features observed in the *K* edges of the Fe and Cu chalcopyrites can be due to interference effects from the atomic structure surrounding the absorber, because the preedge was also observed in the Cu edges, where all the $3d$ states are occupied.

For sake of clarity in analyzing the *M* XANES plots (Figs. 3 and 4), a certain assignment of the near-edge reso-

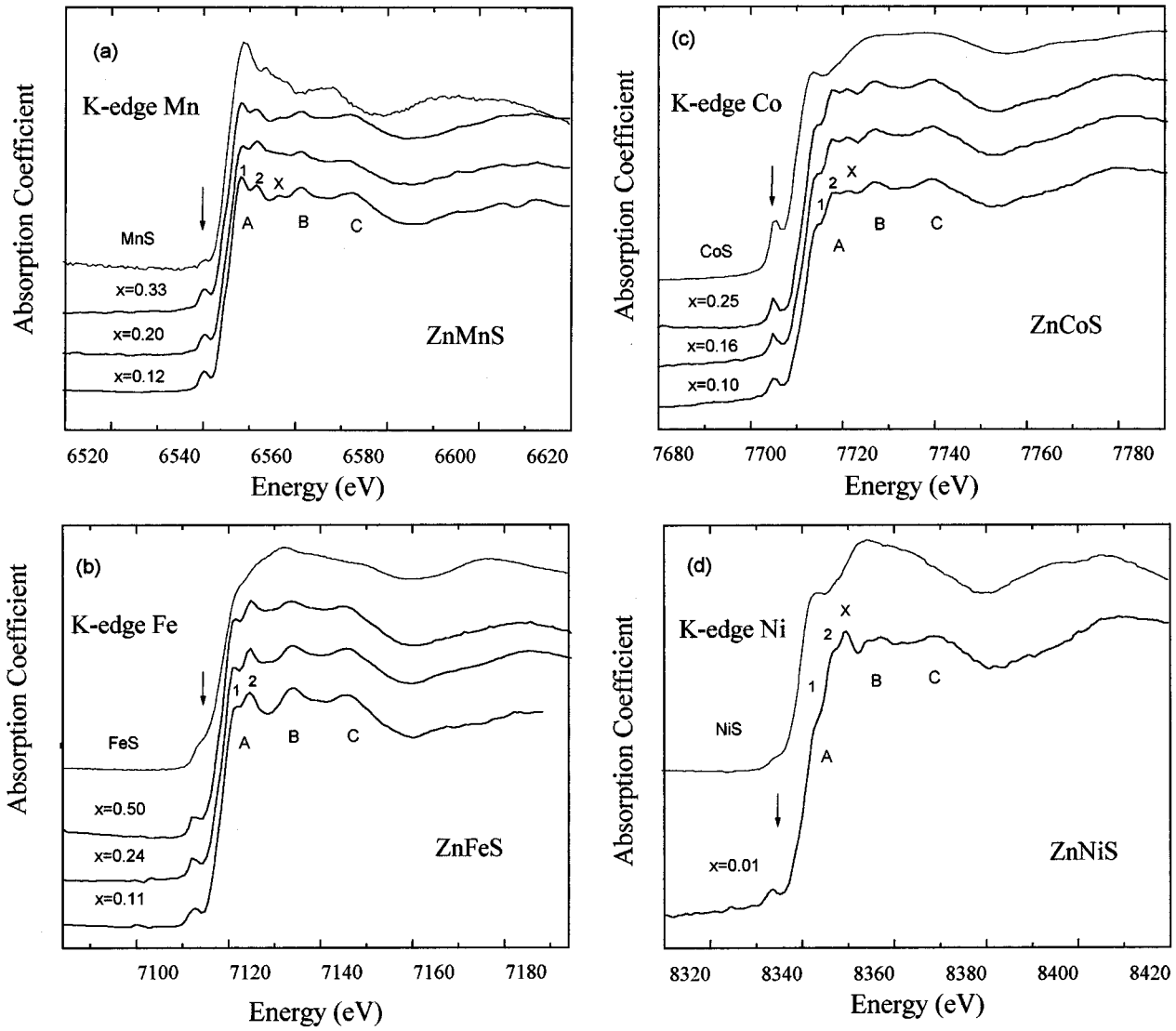


FIG. 3. $K$ edges of $M$ atoms in $MS$ and Zn$MS$ with different content of the following $M$ species: (a) Mn, (b) Fe, (c) Co, and (d) Ni.

nances was introduced. Due to the qualitative similarity of the shape of XANES between Zn- and $M$ $K$-edge spectra for $Zn_{1-x}M_xS$ [compare Figs 1(a) and 3], the peaks of the latter ones were denoted analogously. That is, marks $B$ and $C$ have been used to indicate identical energy distances of the respective peaks from the edge position. Since the feature relevant to resonance $A$ from Fig. 1(a) appears as the split peak in the $M$ $K$-edge spectra [see especially Fig. 3(a)], we have denoted it by $A1$ and $A2$.

The maximum denoted by $A1$ is most pronounced for Mn $K$ edges [Fig. 3(a)]. Going from Mn through Fe and Co to Ni, the intensity of this feature decreases, and in the case of Ni it is only seen as an inflexion at the edge [Fig. 3(d)]. The number of the empty $3d$ states also diminishes with atomic number from Mn to Ni. This indicates that if the $3d$ states of $M$ affect the intensity of the $K$-edge absorption spectra, this influence can be reflected in the shape of the main maximum $A$ rather than in the preedge. Also the intensity of the $A2$ peak changes when passing from Mn to Ni. It reaches a maximum for the Fe dopant [Fig. 3(b)], whereas for Ni the $A2$ remains in residual form as an inflexion point, similarly as to the $A1$ peak [Fig. 3(d)]. Figure 3 also shows that the shapes of the $B$ and $C$ resonances are practically independent of the choice of the $M$ alloyed with ZnS. This is not surprising if we are reminded that most features of the edge structure already appear in the MS calculations after including the first shell of neighbors, and that the amplitude of photoelectron scattering on Zn atoms is relatively small compared to the scattering on S atoms.[30] For low concentrations of $M$, the $M$ absorbing atom has only Zn atoms in the second coordination sphere. With the rise of $M$ content the number of $M$ atoms in the second shell increases, and this can possibly change only the amplitude of resonances.[30] One additional feature of the $M$ XANES spectra in Zn$MS$, that can be distinguished in Fig. 3, is denoted by $X$. Its intensity also depends on the $M$ element—the $X$ peak remains weakly noticeable for Mn and Fe and better pronounced for Co, whereas in the case of Ni it appears as the dominant XANES maximum [Fig. 3(d)].

Analogously to the latter case, an analysis of the $M$ XANES spectra in selenides (Fig. 4) was based on a certain qualitative similarity between their structure and the Zn XANES in selenides given in Fig. 1(b). As above, the first pair of peaks above the edge position was denoted by $A1$ and

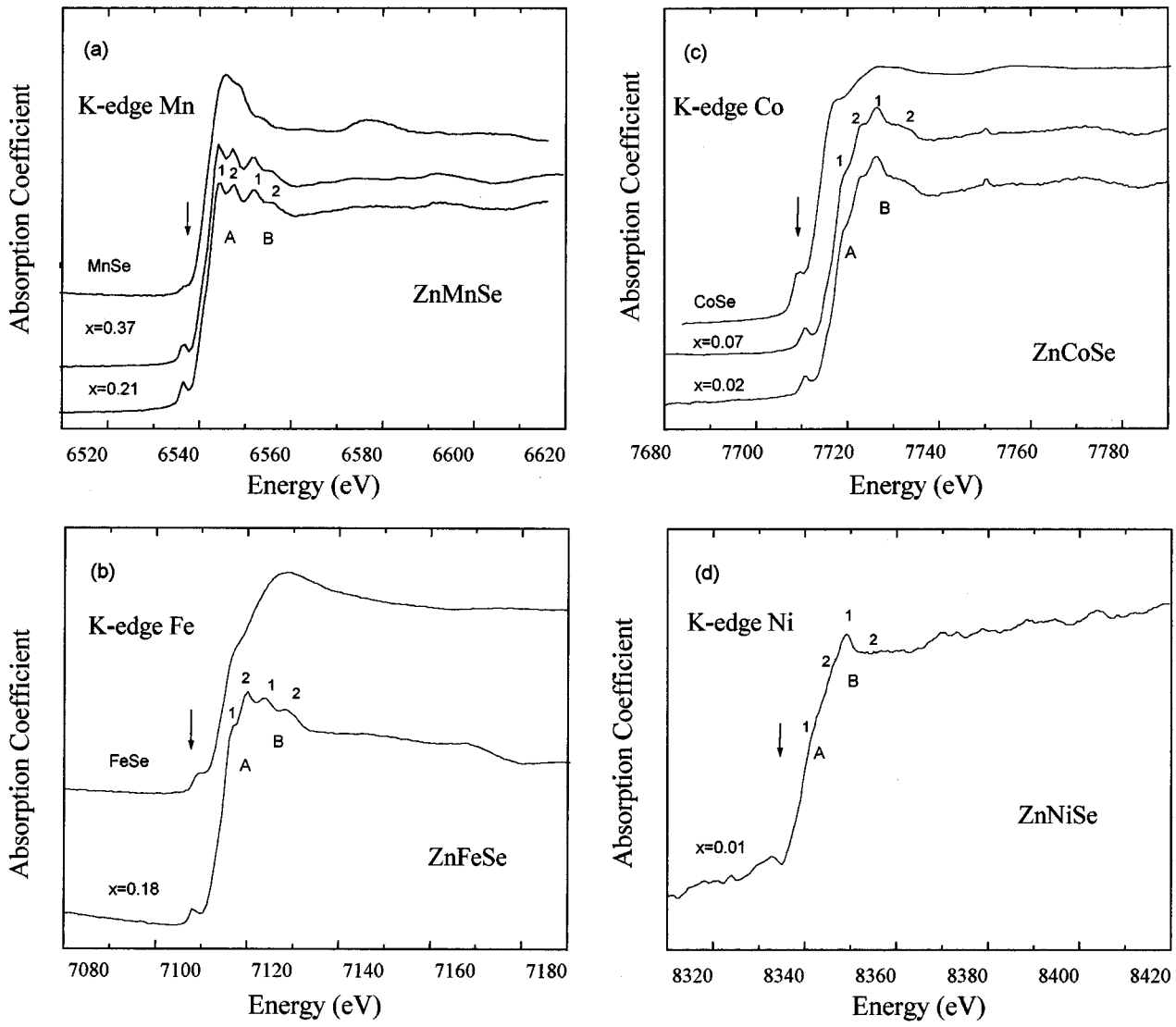


FIG. 4. *K* edges of *M* atoms in *M*Se and Zn*M*Se with different content of the following *M* species: (a) Mn, (b) Fe, (c) Co, and (d) Ni.

*A*2 [see Fig. 4(a)], and the second pair by *B*1 and *B*2, since their position vs edge corresponds to the *B* resonance for the Zn *K* edge [Fig. 1(b)].

Features *A*1 and *A*2 show similar behaviors with the change of *M* from Mn to Ni as in sulfides, when varying from the dominant peaks for Mn to the weak inflection points on the Ni *K*-edge slope. On the other hand, the *B*1 peak tends to increase its intensity when passing from Mn to Ni—for Co and especially for Ni *K*-edge XANES it even becomes a dominant resonance [Figs. 4(c) and 4(d)]. Conversely, the weaker *B*2 feature seems to be damped with the change of *M* down to a complete disappearance for the case of Ni.

It can be concluded from the above analysis of *M* *K*-edge XANES in the sulfides and selenides studied (Figs. 3 and 4) that the most significant differences between the density of *p*-like state distributions of particular transition metals occur very near to the edges, precisely for energies $E-E_0<20$ eV. The most evident change is that the position of the *K*-edge maximum shifts apart from the Fermi level when stepping up from Mn to Ni (see Fig. 5). This can be due (by analogy to the case described in Ref. 17) to the varying slope of the

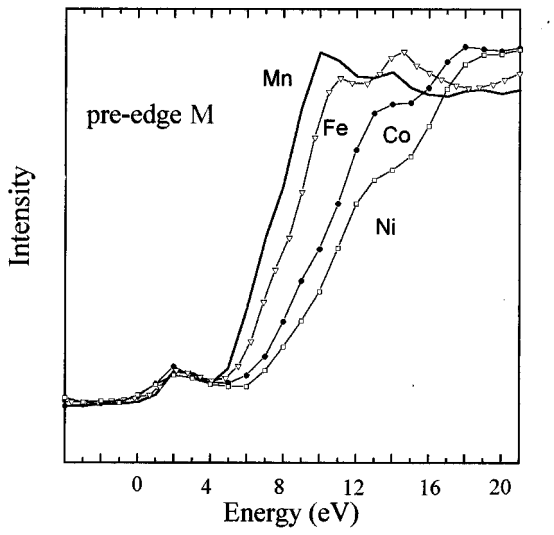


FIG. 5. The *M*-*K* edges in Zn*M*S matrix normalized to their intensities at the near-edge maximum. Zero of the energy scale was shifted to the low-energy edge of the preedge peak.

atomic absorption cross section (for $E>E_0$) when going from Mn to Ni. We have not observed any dependence of the preedge structure on the type and content of $M$—only the dependence on the coordination number was confirmed. The intensity of feature $A$ $(A1, A2)$ changes with filling of the $3d$ shell in $M$, although it does not depend on the type of anion. On the other hand, the photoelectron studies, performed for the DMS based on Zn and Cd chalcogenides,[34–36] revealed the appearance of the $M$ $3d$ partial DOS in the valence-band (VB) region. Its position, approximately 3.5 eV below the VB edge for Mn,[34] shifts upwards toward the VB edge for the case of Fe and Co dopant.[35,36] This could also imply certain shift of the empty $M$ $3d$-related antibonding states in reference to the Fermi level. It is also worth adding here that the first measurements of the $L_3$ edges in ZnS doped with Fe showed that the Fe-related $3d$ antibonding states are split into two peaks separated by 2 eV, and that their intensity changed with the Fe content.[37] The features of $M$ $K$-edge XANES influenced by the $M$ $3d$ states should also change their intensity with the $M$ content. We did not observed such changes, but this can be due to the relatively high lifetime of the $1s$ $M$ level which smooths out the details of the structure. Therefore, the structure of the $A$ peak $(A1, A2)$ of the $M$ $K$ edges studied could be more indicative of the influence of empty $M$-related $3d$ states than the preedge feature.

Additionally, the $K$-edge energies $(E_0)$ for the transition metals (Mn, Fe, Co, Ni) in $Zn_{1-x}M_xS$ and $Zn_{1-x}M_xSe$ alloys were collected in Table II. The position of the $K$-absorption threshold was determined from a maximum of the first derivative within its main slope—a standard procedure for estimating $E_0$ (see, e.g., Refs. 8 and 38). Table II also contains the values of chemical shift $D$, which results from simple subtraction of the $E_0$ of the $M$ in an alloy and in pure $M$. The absolute energies of the transition-metal $K$ edges in the DMS's studied were set by assigning the energy of $K$ edges in pure metals to their known reference values.[39]

The chemical shift depends strongly on charge transfer in the ionic bond and on a number of the nearest neighbors. This has been well described theoretically for transition metals in matrices with ionic bonds by Kitamura and Chen,[40] who performed self-consistent-field calculations of the chemical shift vs charge $(q)$ dependences for different transition metal ions, $(M)^{+q}$.

Judging from the Table II, the value of $D$ is independent of the $M$ content in ZnS and ZnSe. Also, within the accuracy of determining $D$ $(\mp 0.5$ eV), it does not depend significantly on the choice of matrix (here ZnS or ZnSe), although the tendency of slightly smaller $D$ value for selenides can be noticed. This seems rather understandable due to their similar ionicity $[f_1=0.63$ (Ref. 38)]. The magnitude of chemical shifts of $M$ in the DMS's studied ranges within 5–8 eV with a declining tendency when varying the $M$ component in an alloy, from Mn to Ni (see Table II). This indicates, following the calculations of Ref. 40, that the effective charge of $M$ cation remains within $2e-2.5e$. Such a result can be due to the fact that in the case of $M$ cation one could also expect, besides the electrons from $4s$ orbital, a contribution of the $3d$ electrons to the overall charge transfer.

TABLE II. Position of K-absorption thresholds $(E_0)$ for transition metals (Mn, Fe, Co, Ni) in the representative set of $Zn_{1-x}M_xS$ and $Zn_{1-x}M_xSe$ mixed crystals. The absolute energies of the $M$ $K$ edges in the DMS studied were set by assigning the $E_0$ values for elemental metals (marked by *) to their known reference values (Ref. 39). $D$ denotes the chemical shift obtained from subtraction $E_0$ (alloy)$-E_0$ (elem. $M$).

| Material | | $E_0$ (eV) | $D$ (eV) |
|---|---|---|---|
| Mn | | 6539.0* | |
| $Zn_{1-x}Mn_xS$ | $x=0.12$ | 6547.0 | 8.0 |
| | $x=0.20$ | 6547.0 | 8.0 |
| | $x=0.33$ | 6547.0 | 8.0 |
| MnS | | 6544.5 | 5.5 |
| $Zn_{1-x}Mn_xSe$ | $x=0.21$ | 6546.6 | 7.6 |
| | $x=0.37$ | 6547.0 | 8.0 |
| MnSe | | 6545.0 | 6.0 |
| Fe | | 7112.0* | |
| $Zn_{1-x}Fe_xS$ | $x=0.11$ | 7119.5 | 7.5 |
| | $x=0.24$ | 7119.8 | 7.8 |
| | $x=0.50$ | 7119.5 | 7.5 |
| FeS | | 7118.6 | 6.6 |
| $Zn_{1-x}Fe_xSe$ | $x=0.18$ | 7119.0 | 7.0 |
| FeSe | | 7119.0 | 7.0 |
| Co | | 7708.9* | |
| $Zn_{1-x}Co_xS$ | $x=0.10$ | 7716.2 | 7.3 |
| | $x=0.16$ | 7716.2 | 7.3 |
| | $x=0.25$ | 7716.2 | 7.3 |
| CoS | | 7714.6 | 5.7 |
| $Zn_{1-x}Co_xSe$ | $x=0.02$ | 7715.4 | 6.5 |
| | $x=0.07$ | 7716.4 | 7.5 |
| CoSe | | 7714.6 | 5.7 |
| Ni | | 8332.8* | |
| $Zn_{1-x}Ni_xS$ | $x=0.01$ | 8339.7 | 6.9 |
| $Zn_{1-x}Ni_xSe$ | $x=0.01$ | 8337.8 | 5.0 |

### C. X-ray absorption at the S *K* edge

Each anion atom has four nearest neighbors in the crystals studied. Due to the substitution of Zn by $M$ in the cation sublattice the number of each atomic species changes within the nearest neighbors of the anion. This should obviously modify the density distribution of $p$ states around the anion atoms and hence the shape of the anion $K$ edges. The natural width of the $1s$ level of the S atom is much narrower than for the $1s$ level of Se. The changes of $p$-state distributions are then easier to observe in the $K$ edge of S than for Se.

Figures 6(a) and 6(b) present the $K$ edges of S in ZnS, $Zn_xMn_{1-x}S$, and MnS, and ZnS, ZnFeS, and FeS, respectively. It is possible to distinguish there a low-energy part of the XANES spectra $(E-E_0<12$ eV) indicative of the change of the density distribution of $p$ states around the S atom, induced by substitution of Zn by Mn or Fe atoms. The effect is more significant in the case of Fe dopant [Fig. 6(b)]. Within the accuracy of our experiment there is no trace of inflection or shoulder on the main slope of the S edge in the case of ZnS and $Zn_xMn_{1-x}S$, although a weak peak (marked by an arrow) can be distinguished in the case of MnS [Fig. 6(a)], where S is bonded to six Mn atoms. The first feature on the peak $A$ (denoted by $A1$) is more blunt in the ternary

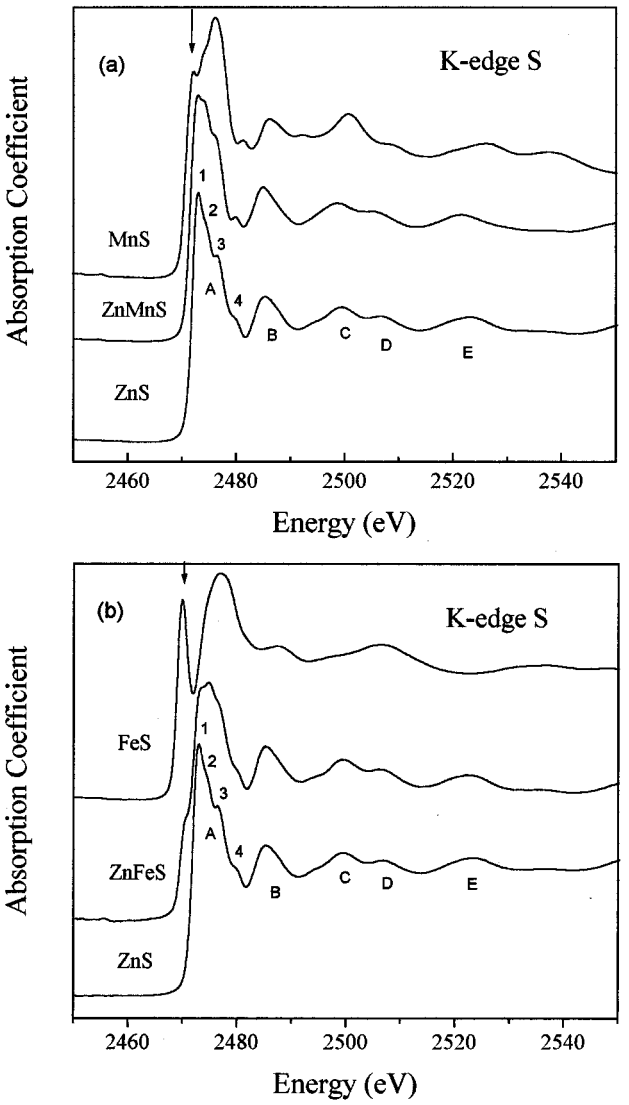


FIG. 6. The $K$ edges of S in $M$S, ZnS, and ZnS doped by particular $M$: (a) Mn, $x=0.33$; and (b) Fe, $x=0.50$.

$Zn_xMn_{1-x}S$ compound whereas the feature $A4$ remains better resolved here than in ZnS. In the case of Fe [Fig. 6(b)] the evident preedge feature appears on the main edge of S in the $Zn_xFe_{1-x}S$ in the same position as the first peak in the XANES of FeS compound (marked by an arrow). For $Zn_xFe_{1-x}S$ the peak $A$ has its maximum at the $A2$ position instead of the $A1$ as in ZnS.

On the other hand, in the higher-energy range of XANES spectra ($E-E_0>12$ eV) the shape and energy positions of the $B$, $C$, $D$, and $E$ resonances do not exhibit qualitative changes with admixing $M$ to the host ZnS (Fig. 6).

The MS theory applied to ZnS (Ref. 30) has shown that due to different values of amplitudes for photoelectron scattering on Zn and S atoms, the single-shell calculation did not describe the characteristic features for the S $K$-edge XANES. Inclusion of the second shell (next-nearest neighbors) reproduced the main XANES structure—nevertheless taking into account eight coordination shells became necessary to reproduce all observed details of ZnS XANES spectra. Therefore, one should not expect significant changes of the S $K$-edge XANES when the first shell is modified by cationic substitution. However, noticeable changes of the structure near to the S $K$ edge were found here. This points out that such changes should be connected with the atomic bound states transitions rather than with interference effects. Pong *et al.*[41] observed variations of the preedge intensity with the $M$ type and concentration. Therefore they have assigned the preedge feature to the $1s$ photoelectron excitation to the S $3p$ states hybridized with $M$ $3d$ $(t_2)$ antibonding states. This suggestion can be supported by our data of Fig. 6(b), where the energy position of the preedge in $Zn_xFe_{1-x}S$ is the same as in binary compound (FeS).

### D. X-ray absorption at the Se *K* edge

The $K$ edges of Se have been measured for all investigated selenides. We do not observe very pronounced changes in the shape of Se $K$-edge XANES (Fig. 7). The Se $1s$ level has a relatively large natural width. It smooths out the fine structure which should be present in the $p$-state distributions. In these edges, one pronounced peak followed by four weaker oscillations can be distinguished. A certain modification of the amplitude of the first resonance and the periodicity of the oscillations can be observed with $M$ content $x$. This effect is especially pronounced for Ni. The rise of Ni content from $x=0.005$ to $x=0.01$ caused a remarkable increase of the amplitude of the first resonance, and even a noticeable shift of the edge energy position, $E_0$ [Fig. 7(d)]. In the case of Mn, relatively higher change of its content (from $x=0.21$ to $x=0.37$) resulted only in weak narrowing of the first resonance [Fig. 7(a)]. This indicates that the modification of the electronic structure around Se induced by Ni atoms is much stronger than by Mn atoms. This can be due to a difference of the scattering amplitude of the emitted photoelectron on the Mn or Ni atom. The solubility limit of Ni in ZnSe is very limited compared to the case of Mn (Table I). We think that different atomic potential of these atoms, in comparison to that of the host cation (Zn), may be the reason why the crystal lattice can easy accommodate a large number of Mn atoms but relatively low concentration of Ni atoms. For comparison, the Se $K$-edge XANES plots from $M$Se binary compounds are presented in Fig. 7. The Se atom has six nearest neighbors in these compounds. The Se $K$-edge XANES for MnSe compound (NaCl structure) exhibits only a single main peak structure, whereas for the rest of monochalcogenides (NiAs structure) the two-peak structure and considerable chemical shift, as compared with the respective ternary compounds, was found. This, together with the presented data of Zn and $M$ XANES, confirms that the number of nearest-neighbor atoms and the type of crystal structure are closely related to the shape of $K$ edge.

## IV. CONCLUSIONS

This paper presents the results of systematic studies of x-ray absorption at the $K$ edges in the XANES range performed for ternary DMS alloys, based on ZnS and ZnSe with transition metal ($M$=Mn, Fe, Co, or Ni) as an admixed element. Our goal was to check how the XANES spectra, and hence the local electronic structure of the alloys studied, can be influenced by a choice and content of $M$ element in cation sublattice or by the choice of anion (S, Se) in Zn compounds.

Analysis of the above data indicates, in agreement with

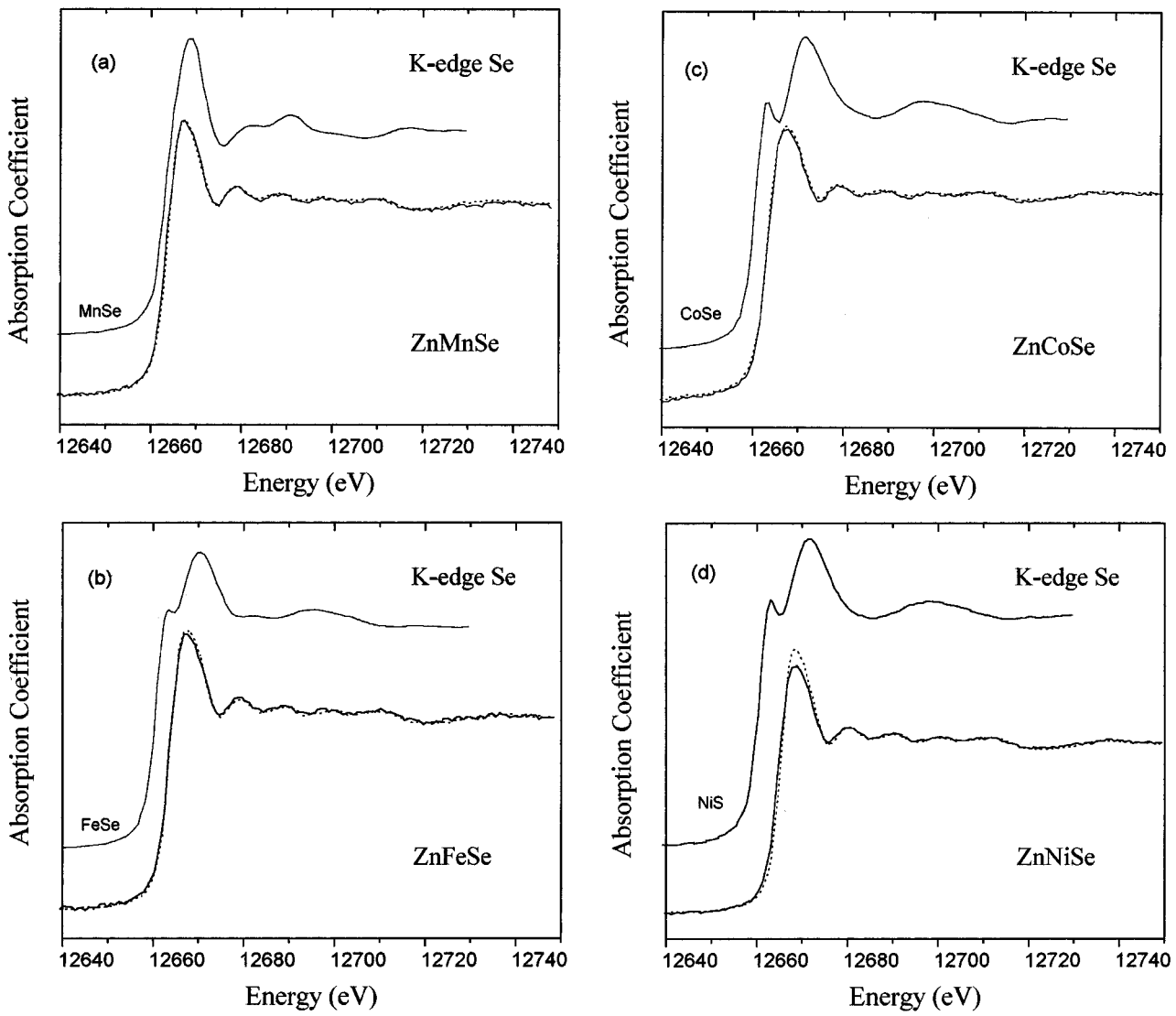


FIG. 7. The $K$ edges of Se in $M$Se and in ZnSe doped by the respective $M$: (a) Mn, dashed line $x=0.37$, solid line $x=0.21$; (b) Fe, dashed line $x=0.18$, solid line $x=0.08$; (c) Co, dashed line, $x=0.07$, solid line, $x=0.02$; and (d) Ni, dashed line $x=0.01$, solid line $x=0.005$.

the respective results of MS theory, that the structure of the cation $4p$-related local DOS's, reproduced by $K$-edge XANES, is mainly determined by the type of anion (first shell). This effect is seen at the Zn $K$-edge absorption spectra, where the three- or two-peaks near-edge structure for sulfides and selenides, respectively, can be distinguished. Also the $M$ $K$ edge XANES show a certain similarity with the host cation (Zn) $K$-edge plots. The observed distinctions between them are due mainly to differences of the atomic absorption cross section of the elements considered. This led us to reveal specific empirical correlation—closer qualitative resemblance between $M$ and Zn $K$-edge XANES corresponds to higher value of solid solubility limit (and vice versa) of a particular $M$ in ZnS or ZnSe. In other words, the best condition to dissolve a particular element in a given solid matrix can be reached when a close similarity between atomic absorption cross sections of substituted and host elements (here $M$ and Zn) occurs. Such correlation results from substitutional-ion-type dependence of the $M$ XANES, which has been evidenced by us for the energies near the main edge position, i.e., $E-E_0<20$ eV. Since the cation XANES spectra were found to be rather weakly dependent on the $M$ content, we conclude that cation substitution within its second-nearest-neighbor shell has a lower order effect and results only in change of the $p$-state localization (amplitude of $K$ edge resonances). This agrees with the prediction of the MS theory that the amplitude of photoelectron scattering on the anion shell is much higher than that on the cation one. Therefore the changes of atomic species distribution within the second coordination shell should not lead to pronounced differences in the XANES.

No evidence of the $M$ XANES preedge dependence on the $M$ $3d$ band filling or $M$ content was found, nevertheless a dependence of the preedge feature shape and intensity on the coordination number was confirmed.

The hybridization effects due to $M$ substitution were found in the anion $K$-edge XANES, although only for sulfur with the $1s$ level sufficiently narrow to obtain small details in the absorption spectra. On the contrary, for Se $K$ edge we failed to distinguish pronounced changes of the XANES shape that could be related to the $M$ substitution in cation sublattice, although some changes of the amplitude of first

resonance due to different magnitudes of the photoelectron scattering amplitude for particular $M$'s were observed.

Generally, our paper is, to our knowledge, the first which reports such complex investigations of $K$-edge XANES for constituent cations and anions for a whole group of II-VI DMS alloys, namely $Zn_{1-x}(M)_xA$ ($M$=Mn, Fe, Co, Ni; $A$=S, Se). Nevertheless, further theoretical studies of the unoccupied $p$-related local DOS's around the Zn, $M$, S, and Se atoms in the investigated DMS compounds, and in the energy range up to 50 eV above the edge, are highly desired.

## ACKNOWLEDGMENTS

This work was supported in part by Grant No. 2 2314 91 02 of the State Committee for Scientific Research (Republic of Poland). The authors would like to express their gratitude to Dr. W. Paszkowicz for the x-ray-diffraction measurements.

[1] J. K. Furdyna, J. Appl. Phys. **64**, R29 (1988).
[2] W. Giriat and J. K. Furdyna, in *Diluted Magnetic Semiconductors*, edited by J. K. Furdyna and J. Kossut, Semiconductors and Semimetals Vol. 25 (Academic, New York, 1988).
[3] A. Twardowski, J. Appl. Phys. **67**, 5108 (1990); in *Diluted Magnetic Semiconductors*, edited by M. Jain (World Scientific, Singapore, 1991), p. 276.
[4] J. Dicarlo, M. Albert, K. Dwight, and A. Wold, J. Solid State Chem. **87**, 443 (1990).
[5] Y. Shapira, in *Semimagnetic Semiconductors and Diluted Magnetic Semiconductors*, edited by M. Averous and M. Balkanski (Plenum, New York, 1991), p. 121; A. Lewicki, A. I. Schindler, J. K. Furdyna, and T. M. Giebultowicz, in *Diluted Magnetic Semiconductors* (Ref. 3), p. 410.
[6] C-M. Niu, R. Kershaw, K. Dwight, and A. Wold, J. Solid State Chem. **85**, 262 (1990).
[7] P. Wu, R. Kershaw, K. Dwight, and A. Wold, Mater Res. Bull. **24**, 49 (1989).
[8] B. K. Teo, *EXAFS: Basic Principles and Data Analysis*, Inorganic Chemistry Concepts Vol. 9 (Springer, Berlin, 1986).
[9] A. Balzarotti, M. Czyzyk, A. Kisiel, N. Motta, M. Podgorny, and M. Zimnal-Starnawska, Phys. Rev. B **30**, 2295 (1984).
[10] A. Balzarotti, N. Motta, A. Kisiel, M. Zimnal-Starnawska, M. T. Czyzyk, and M. Podgorny, Phys. Rev. B **31**, 7526 (1985).
[11] W.-F. Pong, R. A. Mayanovic, B. A. Bunker, J. K. Furdyna, and U. Debska, Phys. Rev. B **41**, 8440 (1990).
[12] R. A. Mayanovic, W.-F. Pong, and B. A. Bunker, Phys. Rev. B **42**, 11 174 (1990).
[13] P. A. Lee, P. H. Citrin, P. Eisenberger, and B. M. Kincaid, Rev. Mod. Phys. **53**, 769 (1981).
[14] A. Kisiel, J. Oleszkiewicz, M. Podgorny, G. Dalba, F. Rocca, and E. Burattini, J. Cryst. Growth **101**, 237 (1990).
[15] A. Kisiel, A-I. Ali Dahr, P. M. Lee, G. Dalba, P. Fornasini, and E. Burattini, Phys. Rev. B **44**, 11 075 (1991).
[16] A. Kisiel, P. M. Lee, E. Burattini, G. Dalba, P. Fornasini, and W. Giriat, Solid State Commun. **81**, 151 (1992).
[17] D. A. McKeown, Phys. Rev. B **45**, 2648 (1992).
[18] J. E. Müller and J. W. Wilkins, Phys. Rev. B **29**, 4331 (1984).
[19] P. Kizler, Phys. Lett. A **172**, 66 (1992).
[20] L. A. Grunes, Phys. Rev. B **27**, 2111 (1983).
[21] E. E. Alp, G. L. Goodman, L. Sodesholm, S. M. Mini, M. Ramanathan, G. K. Shenoy, and A. S. Bommannavar, J. Phys. Condens. Matter **1**, 6463 (1989).
[22] P. Barton and P. Toulmin, Econ. Geol. **61**, 815 (1966).
[23] M. Jain and J. L. Robins, in *Diluted Magnetic Semiconductors* (Ref. 3), p. 1.
[24] Z. Gołacki (private communication).
[25] W. Becker and H. D. Lutz, Mater. Res. Bull. **13**, 907 (1978).
[26] M. Lemmonier, O. Collet, C. Depautex, J.-M. Esteva, and D. Raoux, Nucl. Instrum. Methods **152**, 109 (1978).
[27] A. Bianconi, in *X-Ray Absorption (Chemical Analysis Vol. 92)*, edited by D. C. Koningsberger and R. Prins (Wiley Interscience, New York, 1988).
[28] M. Breinig, M. H. Chen, G. E. Parente, B. Crasemann, and G. S. Brown, Phys. Rev. A **22**, 520 (1980).
[29] K. Ławniczak-Jabłońska and Z. Gołacki, Acta Phys. Pol. A **86**, 727 (1994).
[30] P. Sainctavit, J. Petiau, G. Calas, M. Benfatto, and C. R. Natoli, J. Phys. (Paris) **48**, C9-1109 (1987); P. Sainctavit, J. Petiau, M. Benfatto, and C. R. Natoli, Physica B **158**, 347 (1989).
[31] H. P. Hanson and J. R. Knight, Phys. Rev. **102**, 632 (1956).
[32] G. Sankar, P. R. Sarode, and C. N. R. Rao, Chem. Phys. **76**, 435 (1983).
[33] M. Belli, A. Scafati, A. Bianconi, S. Mobilio, L. Palladino, A. Reale, and E. Burattini, Solid State Commun. **35**, 355 (1980).
[34] R. Weidemann, H.-E. Gumlich, M. Kupsch, H.-U. Middelmann, and U. Becker, Phys. Rev. B **45**, 1172 (1992).
[35] B. A. Orłowski, B. J. Kowalski, and V. Chab, Phys. Scr. **41**, 984 (1990).
[36] K. Ławniczak-Jabłońska, Z. Gołacki, W. Paszkowicz, J. Masek, L.-S. Johansson, and M. Heinonen, J. Phys. Condens. Matter **6**, 3369 (1994).
[37] K. Ławniczak-Jabłońska and R. Perrera (unpublished).
[38] S. V. Adhyapak and A. S. Nigavekar, J. Phys. Chem. Solids **37**, 1037 (1976).
[39] J. A. Bearden and A. F. Burr, Rev. Mod. Phys. **39**, 125 (1967).
[40] M. Kitamura and H. Chen, J. Phys. Chem. Solids **52**, 731 (1991).
[41] W. F. Pong, R. A. Mayanovic, K. T. Wu, P. K. Tseng, B. A. Bunker, A. Hiraya, and M. Watanabe, Phys. Rev. B **50**, 7371 (1994).